Particle Accelerators
1980 Vol.11 pp.161–172
0031-2460/81/1103-0161$06.50/0

© Gordon and Breach, Science Publishers, Inc.
Printed in the United States of America

ELECTRIC FOCUSING IN CYCLOTRONS WITH UNUSUAL DEES*

M. M. GORDON and FELIX MARTI

Cyclotron Laboratory, Michigan State University, East Lansing, Michigan 48824 U.S.A.

(Received October 7, 1980)

Previous analyses of electric focusing are reviewed and found to be restricted to cyclotrons with 180° dees. For dees with smaller angular widths, an alternating-gradient type of focusing occurs because the ions generally enter and exit each dee on opposite sides of the rf voltage peak. This AG focusing effect is analyzed and formulas are derived for calculating the resultant change in ν_z. These formulas are applied first to the MSU superconducting cyclotron, which has three 60° dees, and then to the Indiana cyclotron which has two 38° dees. We find in the first case that electric focusing will be quite significant for certain harmonics, and in the second case that it may even produce a small region of vertical instability through overfocusing. Next, the analysis of Dutto and Craddock is generalized so as to apply to dees with spiral electric gaps like those designed for use in superconducting cyclotrons. Formulas for the resultant change in both ν_r and ν_z are derived, and then applied to the MSU cyclotron with some rather interesting results.

1. INTRODUCTION

During electric gap-crossings, ions in the beam experience vertical focusing forces produced by the same rf field that is responsible for their acceleration. This electric focusing plays an important role near the center of most cyclotrons in a region where the magnetic focusing tends to be very weak and where, simultaneously, the defocusing associated with space-charge repulsion has its greatest strength.

The focusing effects produced by the rf electric field in classical cyclotrons were analyzed first by Rose[1] and Wilson,[2] and later with some refinements by Cohen.[3] Since then, this analysis has been revised and extended to isochronous cyclotrons by a number of authors.[4,5] As a result, most aspects of the phenomena are now well understood.

Before proceeding, it seems worthwhile to review briefly some important properties of electric focusing. First, the time dependence of the forces leads inevitably to a vertical acceptance for the cyclotron that depends on the phase of the injected ions (whether from an internal or external source). Moreover, it turns out that this phase dependence differs substantially from that of the energy gain per turn.

These conflicting characteristics tend to limit considerably the phase acceptance, as well as the vertical acceptance of most cyclotrons. Within these limitations, the ultimate performance can nevertheless be significantly improved by means of suitable design procedures, as pointed out by several investigators.[6]

To understand the basic phenomena, one should first recognize the electric lenses which accelerate ions across a gap generally produce a focusing impulse as the ions enter the gap and a defocusing one as they exit. These opposing impulses result from the curvature of the electric field lines, which is illustrated, for example, in Fig. 1.

The primary focusing effect in cyclotrons, called the "phase effect", is produced by the time variation of the dee voltage. Here for example, if the ion crosses the gap at a time when the field strength is falling, then the focusing impulse will exceed the defocusing one, and a net focusing will result. Conversely, if the crossing occurs when the field strength is rising, then a net defocusing is produced. This phase effect turns out to be inversely proportional to the turn number, and moreover, the result is essentially independent of the electric-field variation within the gap.

The secondary focusing effects in cyclotrons are almost exactly the same as those associated with static electric lenses. These are the well-known "acceleration" effect and the "thick-lens" effect, which always yield a net focusing

* This material is based on work supported by the National Science Foundation under Grant No. Phy 78-22696.

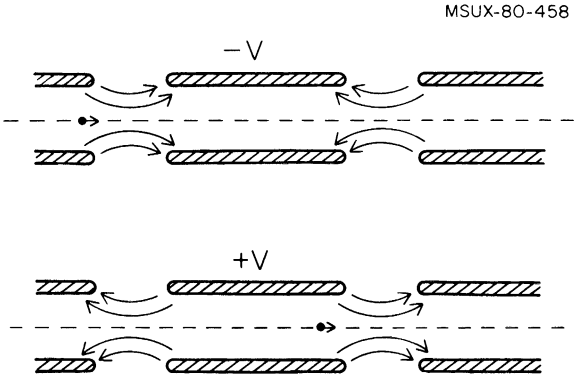

FIGURE 1 Side view of central-ray orbit which, for simplicity, has been unwound and laid out straight. Top drawing shows one particle entering the dee at a time when the dee's relative potential is $-V$. Bottom drawing shows same particle about to exit this dee when its relative potential is $+V$. The curved arrows indicate the electric-field lines within the two gaps that bound the dee.

result for the complete lens. These effects generally fall off more rapidly with turn number than the phase effect, and are therefore comparable in significance only during the first turn or so.

The analyses mentioned in the second paragraph above have all been carried out for cyclotrons having two gap-crossings per turn, which corresponds to 180° dees. But many cyclotrons have now been designed with four, six, or even eight gap-crossings per turn and with a wide variety of dee angles.[7] In such cases, these ions that gain the maximum energy per turn generally enter and exit each dee on opposite sides of the rf voltage peak, where they experience equal focusing and defocusing impulses. As one would expect, the net result is a focusing effect, which may therefore be called "alternating-gradient" focusing.

After developing in Sec. 2 the necessary relationship between energy gain and phase, we proceed in Sec. 3 to analyze this alternating-gradient effect and to obtain suitable formulas for calculating the resultant ν_z values. These formulas are applied first in Sec. 4 to the 500-MeV superconducting cyclotron nearing completion here at MSU, and then in Sec. 5 to the low-energy cyclotron ring used as an injector at Indiana.

All of the previous analyses have also assumed a relatively simple model based on a Cartesian geometry with the central-ray orbit moving in a straight line directly across each gap. Such a model is reasonably appropriate for 180° dees, but it seems much less suitable for the narrower dees considered here, where in general, the angular width of the gaps as well as the dees is nearly constant. To remedy this situation, we present in Sec. 6 an analysis of electric focusing using a polar-coordinate geometry.

Our approach is based on a modification of the rather neat analysis developed by Dutto and Craddock.[5] We include in our results a revised version of their complementary relationship between radial and vertical focusing, and then apply these results in Sec. 7 to the spiral electric gaps now widely used in the design of superconducting cyclotrons. As we shall show, the differential focusing effect produced by such gaps can either decrease ν_r and increase ν_z, or vice versa, depending on whether the ions are moving "against" or "with" the curvature of the spiral gaps.

Our general aim here is to obtain simple analytical formulas that can be used first to estimate electric-focusing effects during preliminary design work, and can also be used later as a guide to interpreting the numerical data from some sophisticated computer program.

2. ENERGY GAIN

Before proceeding, we need to obtain a relationship between the energy gain at a particular gap crossing and the phase ϕ of an ion being accelerated in a cyclotron having a quite-general dee configuration. In conformity with the precedent established by Rose,[1] and followed thereafter by most (but not all) cyclotron designers, we define ϕ by

$$\phi = \omega_{rf} t - h\theta - \kappa , \tag{1}$$

where $h = \omega_{rf}/\omega_0$ is the integral harmonic ratio of the rf frequency to the (ideal) orbital frequency. The constant κ is determined by requiring that the energy gain per turn be given by

$$\Delta T = \int q\mathbf{E} \cdot \mathbf{ds} = qV_1 \cos\phi , \tag{2}$$

where V_1 is then the peak voltage gain per turn.

This definition of ϕ differs from that commonly used in treatments of synchrotron oscillations, which follow the convention originally adopted by McMillan.[8] These two definitions are connected by the relation

$$\phi_{syn} = \frac{\pi}{2} - \phi_{cyc} . \tag{3}$$

It is interesting to note, however, that Kolomensky and Lebedev[9] use the same definition as in Eqs. (1) and (2) above, and it seems likely that they are following the lead of Veksler.[8]

Suppose that the cyclotron is equipped with a set of N_d identical dees, and for the sake of symmetry, assume that these are uniformly spaced with a constant interval

$$\theta_e = 2\pi/N_d \,. \tag{4}$$

Suppose further that the voltage on the ith dee relative to its surroundings (dummy dee or liner) is given by

$$V_{di} = V_0 \sin(\omega_{rf} t - k_i) \,, \tag{5}$$

with successive values of $i = 1, 2, \ldots, N_d$ being in the order in which the ions traverse the dees. Here V_0 is the nominal dee voltage, and k_i is the rf phase of the ith dee.

Next, let D be the angular width of each dee where, of course, $D < \theta_e$, given in Eq. (4) above. There are then $2N_d$ gap-crossings per turn, and we can take their successive positions to be given by

$$\theta_{ij} = i\theta_e + (-1)^j D/2 \,, \tag{6}$$

where $j = 1$ or 2 specifies, respectively, whether the ion is entering or exiting the ith dee.

In accordance with the picture in Fig. 1 and the dee voltage given in Eq. (5), we then find that the energy gained by the ion while entering or exiting the ith dee is given by

$$\delta T_{ij} = (-1)^j q V_0 \sin(\phi + \kappa + ih\theta_e - k_i + (-1)^j hD/2) \,, \tag{7}$$

where use has been made of the definition of ϕ in Eq. (1) as well as θ_{ij} in Eq. (6). Adding these energies together, we then obtain

$$\delta T_{i1} + \delta T_{i2} = 2qV_0 \sin(hD/2) \cdot \cos(\phi + \kappa + ih\theta_e - k_i) \,, \tag{8}$$

which is the total energy acquired by the ion in traversing the ith dee.

It is clear from the symmetry that this energy gain must be the same for all dees. Furthermore, it must be proportional to $\cos\phi$ in order to satisfy the condition imposed by Eq. (2) for ΔT. It therefore follows that k_i must be given by

$$k_i = ih\theta_e + \kappa \,, \tag{9}$$

which, as might be expected, simply requires that as the ion circulates from one dee to the next, the change in voltage phase must be h times the angular distance θ_e covered by the ion.

The total energy gain per turn is then given by

$$\Delta T = 2N_d q V_0 \sin(hD/2) \cos\phi \,, \tag{10}$$

and comparing with Eq. (2), it also follows that

$$V_1 = 2N_d V_0 \sin(hD/2) \tag{11}$$

is the corresponding expression for the voltage gain per turn. Since it is customary to treat both V_1 and V_0 as positive constants, we shall henceforth assume that $(hD/2)$ is evaluated modulo π.

Returning to the expression (7) for the energy gained by the ion on entering or exiting the dee, and making use of Eq. (9), we then find

$$\delta T_j = + qV_0 \sin(\tfrac{1}{2}hD + (-1)^j \phi) \,, \tag{12}$$

where the subscript i can now be dropped. Thus when $\phi = 0$, the ion gains the same energy at both gaps, in accordance with an old rule-of-thumb.

Excepting the case where $D = 180°$, this result also shows that the ion crosses the gaps on the "sides" of the rf voltage peak and that when $\phi \neq 0$, it gains more energy from one gap than from the other. Indeed, when the magnitude of ϕ approaches 90°, the ion will actually lose energy at one gap while gaining enough at the other end to end up with a net energy gain.

Finally, we should note that for $D = 180°$, and h odd, the above formula reduces to

$$\delta T_1 = \delta T_2 = qV_0 \cos\phi \,, \tag{13}$$

which coincides with the old widely used formula for a standard dee geometry.

3. ALTERNATING-GRADIENT FOCUSING

In evaluating the electric focusing produced by the dees, the problem can be greatly simplified if we make use of the results obtained by Dutto and Craddock.[5] We shall defer any detailed discussion of their analysis until Sec. 6, and simply

quote here the part of their results that we need for the present.

The vertical impulse δp_z that the ion receives when it crosses one electric gap can be expressed as

$$\frac{\delta p_z}{m\omega z} = \frac{h}{2T_c}\frac{\partial}{\partial\phi}(\delta T) , \tag{14}$$

where T_c is its kinetic energy at the center of the gap. Of the various focusing effects mentioned in the introduction, this expression corresponds to the result obtained when only the "phase effect" is considered.

For our purposes, the supreme virtue of the above expression lies in its independence of the detailed form of the electric field or of its time dependence, provided only that this field is a function of $\omega_{rf}t$, and that $d\phi = \omega_{rf}\, dt$ when $d\theta = 0$. The latter requirement is evidently fulfilled by the definition of ϕ in Eq. (1).

The energy gain δT_1 and δT_2 at the two gap crossings per dee is given by Eq. (12), and differentiation then yields

$$\begin{aligned}\frac{\partial}{\partial\phi}(\delta T_j) &= (-1)^j qV_0 \cos(\tfrac{1}{2}hD + (-1)^j\phi) ,\\ &= -qV_0 \sin(hD/2)\sin\phi \\ &\quad + (-1)^j qV_0 \cos(hD/2\cos\phi .\end{aligned} \tag{15}$$

As we shall see, the first term here leads to ordinary focusing, while the second term produces AG focusing.

If T_0 is the average value of the energy before and after the ion completely traverses the dee, then the energy at the center of each gap is given by

$$\begin{aligned}T_j = T_0 &- \tfrac{1}{2}qV_0 \cos(hD/2)\sin\phi \\ &+ \tfrac{1}{2}qV_0(-1)^j \sin(hD/2)\cos\phi .\end{aligned} \tag{16}$$

The resultant T_1 and T_2 are the proper values to substitute for T_c in Eq. (14) when evaluating the impulse at the two gaps.

Since Eq. (14) involves a ratio of quantities that are linear in the kinetic energy, we should expect that the resultant focusing will be independent of the absolute value of qV_0. To remove this parameter from further consideration, we replace the energy variable T_0 by the turn number n defined by

$$n = T_0/qV_1 , \tag{17}$$

where qV_1 is the peak energy gain per turn given in Eq. (11). Of course, n is the actual turn number only if $\phi = 0$.

Since we have adopted a formulation based exclusively on the phase effect, we cannot expect our results to be valid within the first turn, that is, for $n < 1$. On the other hand, the accuracy of our results should improve continuously as the value of n increases. In order to be specific, we take $n = 1$ as our lower limit, using as justification the fact that Dutto and Craddock found that their results were still reasonably good down to this limit.

In order to simplify our presentation, we shall assume that $\frac{1}{2}$ is negligible compared with $2nN_d$, or equivalently, that $\frac{1}{2}qV_0 \ll T_0$. With these considerations in mind and making use of Eqs. (15, 16, 17), we finally obtain

$$\beta_j = \frac{-h}{4nN_d}(\sin\phi - (-1)^j \cot(hD/2)\cos\phi) , \tag{18}$$

where $\beta_j = (\delta p_z)/m\omega z$, as given in Eq. (14).

We now proceed to calculate the effect of these impulses on the focusing frequency ν_z. To simplify the calculation, we assume that between gap crossings the vertical oscillations are described by

$$(d^2z/d\theta^2) + \nu^2 z = 0 , \tag{19}$$

where $\nu_z = \nu$ here is the frequency resulting from whatever magnetic focusing is present.

If the ion enters the dee at θ_1 and exists at $\theta_2 = \theta_1 + D$, then the electric-focusing impulses provide the following boundary condition at $\theta = \theta_j$

$$\delta(dz/d\theta) = \beta_j z_j , \tag{20}$$

where β_j is given above. Although the general solution of the differential equation including this boundary condition can readily be obtained, we omit the details for the sake of brevity.

It has become customary in electric-focusing calculations to assume artificially that the focusing forces are periodic with a period $\theta_e = 2\pi/N_d$, which then constitutes an electric "sector." This

assumption makes it possible to construct a transfer matrix for one such sector, and hence to interpret the results directly in terms of a change in ν_z. When this process is carried through, we obtain the following result

$$\cos(\nu_z\theta_e) = \cos(\nu\theta_e) + \frac{\beta_1 + \beta_2}{2\nu}\sin\nu\theta_e + \frac{\beta_1\beta_2}{2\nu^2}\sin\nu(\theta_e - D)\sin\nu D\ , \tag{21}$$

where ν_z here represents the resultant focusing frequency when the electric focusing is included.

If we take the limit where $\nu\theta_e < 1$ and $\nu_z\theta_e < 1$, then the above expression simplifies to

$$\Delta\nu_z^2 = -((\beta_1 + \beta_2)/\theta_e) - (\beta_1\beta_2/\theta_e^2)(\theta_e - D)D\ , \tag{22}$$

where $\Delta\nu_z^2 = \nu_z^2 - \nu^2$. Note that both the exact and the approximate expressions contain one term involving $(\beta_1 + \beta_2)$ and a second involving $\beta_1\beta_2$. The former corresponds to ordinary focusing, while the latter contains the AG focusing.

If we now insert the values of β_1 and β_2 given in Eq. (18) above, we then obtain

$$\Delta\nu_z^2 = \left(\frac{h}{4\pi n}\right)\sin\phi + \left(\frac{h}{8\pi n}\right)^2 (\cot^2(hD/2)\cos^2\phi - \sin^2\phi)(\theta_e - D)D\ . \tag{23}$$

Here the first and second terms correspond to the ordinary and AG focusing, respectively, while the third term represents a thick-lens effect.

Except for $\phi \simeq 0$, the first term becomes predominant as the turn number n increases. Interestingly enough, this term is completely independent of the dee geometry inasmuch as it depends only on h/n.

As can be seen, the alternating-gradient term will be important when h/n is not too small, or when $\phi \simeq 0$. We should also point out that because of the $\cot^2(hD/2)$ factor, this term vanishes when $D = 180°$, while for small D values it becomes most significant for those harmonics h where the voltage-gain per turn V_1 in Eq. (11) has its smallest values.

Finally, it should be noted that the above ν_z value represents a lower limit to the focusing frequency. That is, our analysis has neglected completely the "acceleration" and "thick-lens" effects, which, as noted in the introduction, always produce some additional focusing.

4. MSU SUPERCONDUCTING CYCLOTRON

As an application of the foregoing theory, we consider the central region of the 500-MeV superconducting cyclotron now under construction at MSU.[10] This cyclotron is equipped with three dees, each having an angular width $D = 60°$, as shown schematically in Fig. 2. Here we have $\theta_e = 2\pi/3$ for the period of one electric sector.

Although the rf system is designed to operate on all harmonics, we restrict ourselves here to those of greatest practical interest, namely, $h = 1$ to 5. In each case, the relative importance of AG focusing can be determined simply by examining the factor $\cot^2(hD/2)$ occurring in Eq.

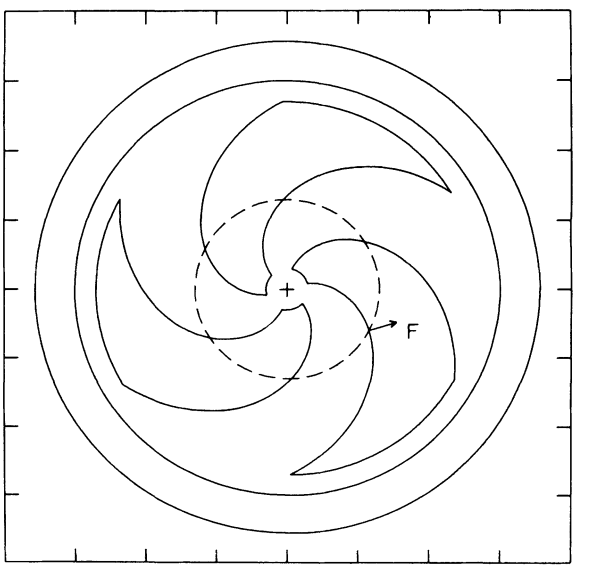

FIGURE 2 Schematic diagram of the median-plane layout in the 500-MeV superconducting cyclotron at MSU. The curved lines coming out from the center indicate the spiral electric gaps bounding the three dees which have a constant angular width $D = 60°$. The broken circle (at $r = 13$ in.) represents the orbit of an ion that, during its counterclockwise rotation, experiences the electric force indicated by F at one particular gap crossing. The two outer circles at $r = 30$ and 36 in. mark the boundaries of the superconducting coils that encircle the poles. These circles serve to demonstrate the compactness of this cyclotron.

(23) for $\Delta\nu_z^2$. As h ranges from $h = 1$ to $h = 5$, this factor takes on the values: $3, \frac{1}{3}, 0, \frac{1}{3}, 3$. Thus AG focusing is most important for $h = 1$ and 5, and is completely absent for $h = 3$.

In order to reveal the strength of the electric focusing most clearly, we start by assuming that magnetic focusing is completely absent. Hence, we let $\nu \to 0$ in Eq. (21), and thereby obtain

$$\cos\nu_z\theta_e = 1 + \tfrac{1}{2}(\beta_1 + \beta_2)\theta_e + \tfrac{1}{2}\beta_1\beta_2(\theta_e - D)D , \tag{24}$$

where $D = \theta_e - D = \pi/3$ in our case. Here we used exact expressions for β_1 and β_2 in the computations described below, rather than the approximate values shown in Eq. (18).

Figure 3 presents a plot of the calculated ν_z values as a function of the phase ϕ for each h value at the end of the first turn ($n = 1$). Only the real values of ν_z are shown, since the defocusing represented by imaginary values could not be tolerated in practice. As can be seen, the values of ν_z generally increase with h, particularly for $\phi > 10°$. This behavior results from β_j in Eq. (18) being proportional to h, except for the AG focusing term.

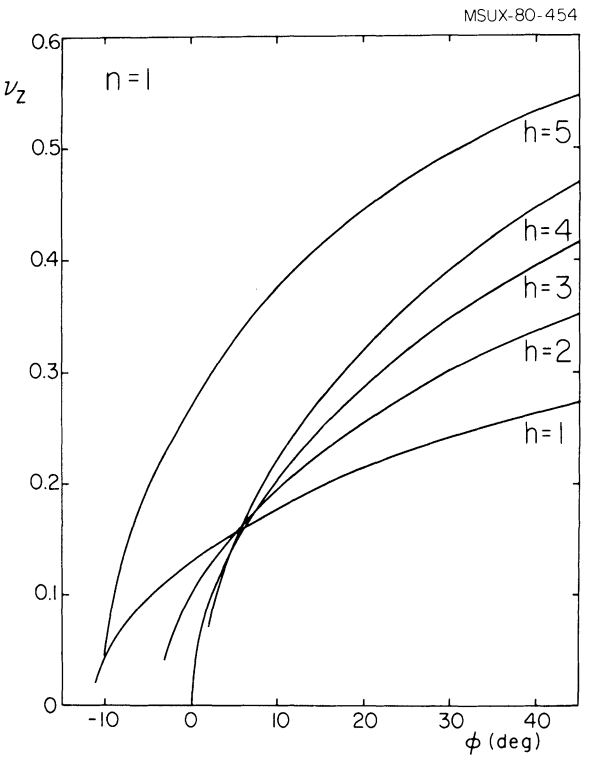

FIGURE 3 Curves showing the theoretical values of ν_z as a function of ϕ obtained exclusively from the electric focusing produced by three 60° dees, like those shown in Fig. 2. All values correspond to conditions at the end of the first turn ($n = 1$), with separate curves for $h = 1$ to 5 to show the dependence on harmonic number. The effect of AG focusing is most pronounced for $h = 1$ and 5 as evidenced by the ν_z values for $\phi < 10°$.

The AG focusing effect becomes appreciable only for $\phi < 10°$, which explains the erratic dependence of ν_z on h shown in this phase range. In particular, for $\phi < 0$, real values of ν_z can be obtained only if the AG focusing is strong enough to overcome the ordinary defocusing. This explains the behavior shown for $\phi = 0$, where the values found for $h = 1$ turn out to be larger than those for $h = 2$, 3, or 4.

The curves in Fig. 3 have been terminated at $\phi = 45°$ even though higher ϕ values would produce larger ν_z values, and hence a greater vertical acceptance. The reason for this termination originates in the $\cos\phi$ dependence of the energy gain per turn. That is, for $\phi > 45°$ or thereabouts, the ions would not gain enough energy on the first turn to clear the ion source or inflector.

The decrease in ν_z with increasing turn number n is shown in Fig. 4 for a fixed phase $\phi = 15°$. To avoid clutter, we present curves only for $h = 1$, 3, and 5, since those for $h = 2$ and 4 fall in their natural places and provide little additional information.

As shown in Fig. 4, the values of ν_z for $h = 5$ remain close to a factor of two larger than those for $h = 1$ for all n values. However, the ratios of the $h = 3$ values to those for $h = 1$ generally increase with n. This behavior can be understood qualitatively by recognizing first that the AG focusing falls off faster with n than the ordinary focusing, and, as noted above, the AG focusing effect is strong for $h = 1$ and $h = 5$, but is completely absent for $h = 3$.

We turn next to consider a comparison of the theory with some data that might be called "experimental." These data represent some very preliminary results obtained with a new computer program "3D-Cyclone", which is designed to calculate three-dimensional orbits in the central region of our superconducting cyclotron using time-dependent electric fields derived from electrolytic-tank measurements.[11]

The following short table presents for comparison values of ν_z labelled "exp" and "thy" which were obtained, respectively, from the aforementioned data and from the theoretical for-

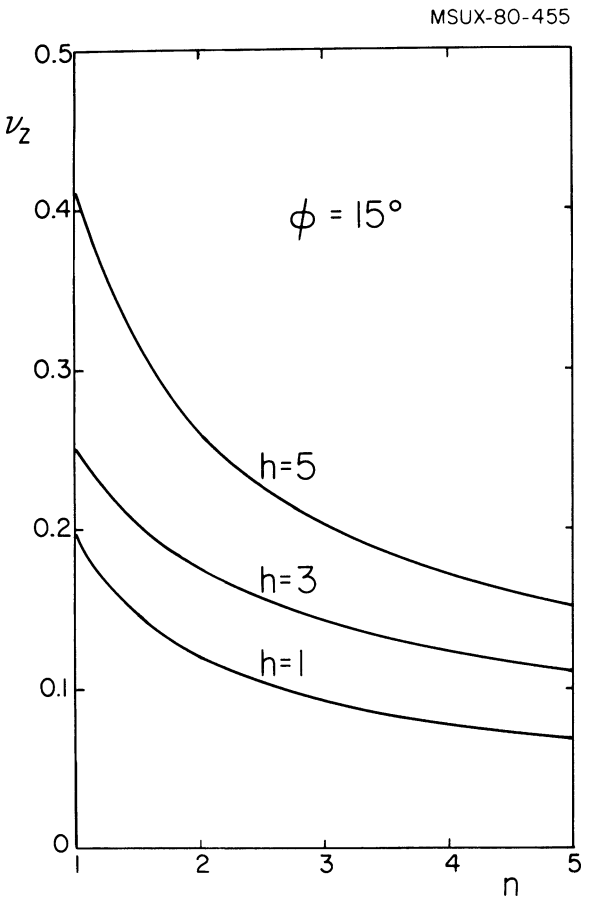

FIGURE 4 Curves showing the decrease in ν_z with increasing turn number n for harmonics h = 1, 3, and 5, and for a fixed phase ϕ = 15°. These curves were obtained from calculations assuming the same dee geometry as that used for the curves in Fig. 3, and therefore represent an extension of those curves.

mulas. Here we can no longer assume that the magnetic focusing is negligible and we therefore include the focusing frequencies (labeled "ν" in the table) derived from measured magnetic-field data using a standard equilibrium-orbit code. These magnetic-focusing frequencies were then combined with the corresponding electric values obtained from our theoretical formulas to provide the final ν_z values listed in the table under the "thy" heading.

n	ϕ	ν	thy	exp
1	20°	0	0.21	0.20
2	18°	0.045	0.14	0.17
3	15°	0.065	0.11	0.17
4	12°	0.095	0.12	0.16

The agreement between the "exp" and "thy" values is fairly good, considering that the theory provides only a lower limit to the ν_z values, as noted at the end of the previous section. We should also mention that the values of n and ϕ in this table were determined from the orbits computed with the 3D-Cyclone program, and that these orbits also show that n = 4 corresponds approximately to a radius r = 2 inch. Beyond this radius, the magnetic focusing produced by the spiral pole tips grows progressively stronger while the electric focusing rapidly diminishes.

5. INDIANA CYCLOTRON

As a second example, we consider the Indiana accelerator, which consists of two cyclotron rings operating in succession, so that the low-energy ring serves as the injector for the high-energy one. Both cyclotrons have four magnet sectors and two dees with D = 38° occupying opposite valleys.

These cyclotrons are designed to operate over a broad spectrum of harmonics, namely, h = 3 to 8, and h = 11 to 17.[12] Again, using the factor $\cot^2(hD/2)$ as a basis for judgment, we conclude that the AG contribution to electric focusing will be largest for h = 8, 11, and 17, and will be smallest for h = 5 and 14.

Generally speaking, separated-sector cyclotrons are characterized by exceptionally strong magnetic focusing and unusually high injection energies.[13] One might therefore expect that electric focusing would play an insignificant role in such cyclotrons. But this expectation appears to be unjustified for the low-energy ring at Indiana, which turns out to be very sensitive to small perturbations of the vertical oscillations.

This sensitivity is brought about by somewhat insufficient magnetic focusing in the region just beyond the injection radius, which causes ν_z to move rather slowly up across the ν_z = 1 resonance line.[14] As is well known, small vertical forces having a cosθ dependence will induce coherent vertical oscillations in the beam during passage through this resonance. Such oscillations are routinely observed at Indiana, and appropriate countermeasures are carried out to effectively cancel their effects.

It should also be recognized that since ν_z = 1 coincides with the parametric resonance $2\nu_z$ = 2, a perturbation of the focusing strength having

a cos2θ dependence can cause the beam to accelerate through a stop-band region wherein the amplitude of the vertical oscillations grows exponentially. It is just such a perturbation that is produced by the electric-focusing forces.

In order to investigate this particular effect, it proves most appropriate to combine the complete expression (21) for ν_z with the approximate equation (18) for β_j. When this is done, we find

$$\cos\pi\nu_z = \cos\pi\nu - \left(\frac{h}{8n\nu}\right)\sin\pi\nu\sin\phi - \frac{1}{2}\left(\frac{h}{8n\nu}\right)^2(\cot^2(hD/2)\cos^2\phi - \sin^2\phi) \cdot \sin\nu(\pi - D)\sin\nu D\ , \quad (25)$$

where we have set $N_d = 2$, $\theta_e = \pi$, and where $D = 38°$ here. Once again we note that ν is the vertical-oscillation frequency produced exclusively by the magnetic focusing, while ν_z is that resulting from the combined effect of both electric and magnetic focusing.

For simplicity, we shall assume $\phi = 0$, since this value eliminates everything from the above equation except the AG focusing term. In this case, we have

$$\cos\pi\nu_z = \cos\pi\nu - \frac{1}{2}\left(\frac{h}{8n\nu}\right)^2 \cdot \cot^2(hD/2)\sin\nu(\pi - D)\sin\nu D\ . \quad (26)$$

Evidently, when $\nu = 1$, we obtain $\cos\pi\nu_z < -1$, and hence a complex value for ν_z, which is characteristic of a stopband.

The extent of this stopband depends on the variation of ν with turn number n in the neighborhood of the resonance, as well as on h. Within the stopband, we can set

$$\nu_z = 1 \pm i\mu\ , \quad (27)$$

where the resultant μ value determines the strength of the instability. For example, if μ is constant, then as θ increases, the amplitude of the oscillations will tend to grow exponentially by the factor: $\exp\mu\theta$.

As a good example, we consider some data supplied to us from Indiana regarding the operation of the low-energy ring on the harmonic $h = 8$, which, as noted above, we expect to be strongly affected by AG focusing. In this case, protons are injected at the radius $r_i = 9.36$ in. with an energy $T_i = 215$ keV, and are extracted finally at $r_f = 40.4$ in. with energy $T_f = 2.83$ MeV. In addition, the dee voltage is set at 28 kV so that the voltage gain per turn is $V_1 = 53$ kV, as determined from Eq. (11). As a result, the protons execute about fifty turns between injection and extraction.

To complete our data requirements, we also obtained a table of values for the frequency ν as a function of the orbit radius r appropriate to this case. Since the formula for ν_z given above involves the turn number n rather than r, we related these variables by recognizing that for an isochronous cyclotron operating under non-relativistic conditions, the energy and hence n are proportional to r^2. Thus we write

$$n = (T_i/eV_1)(r/r_i)^2 = (4.0)(r/9.36)^2\ , \quad (28)$$

where the given numbers are the ones cited above.

Figure 5 shows a plot of the resultant $(\nu - 1)$ values over the narrow range of turn numbers of interest to us here, namely, from $n = 4$ to $n = 12$. As can be seen, the magnetic focusing frequency passes through the resonance value $\nu = 1$ close to $n = 6$, which is just two turns after injection.

These data were then used in Eqs. (26) and (27) above to compute, as a function of n, the values of $(\nu_z - 1)$ or, within the stop-band, the values of μ. These quantities are also plotted in Fig. 5.

As shown in this figure, the protons are injected in the middle of the stop-band and remain there from $n = 4.0$ to $n = 8.6$, where the value of μ drops to zero. Beyond this point, ν_z becomes real, and as n increases further, we find that the $(\nu_z - 1)$ curve rapidly approaches that for $(\nu - 1)$ as the strength of the electric focusing falls off toward zero.

As noted above, the amplitude of the vertical oscillations tends to grow exponentially within the stop band. Since μ is evidently not constant in our case, this growth can be estimated through the formula

$$G = \exp\left(\int \mu d\theta\right) = \exp\left(\int 2\pi\mu dn\right)\ , \quad (29)$$

where the integration extends from the initial turn number $(n = 4.0)$ to the final one $(n = 8.6)$. Using the numerical data depicted in Fig. 5, we finally

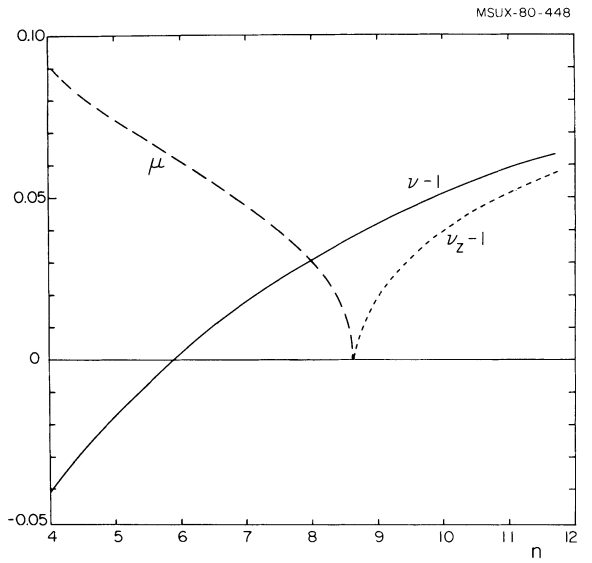

FIGURE 5 Behavior of the vertical-focusing frequency within and beyond the stopband associated with the parametric resonance $2\nu_z = 2$, which is predicted to occur in the low-energy ring at Indiana as a result of electric focusing. These calculations apply specifically to operation of the cyclotron on harmonic $h = 8$ in a case where the protons are injected with 215 keV (corresponding to turn $n = 4$), are accelerated with 53 keV per turn, and finally extracted with 2.83 MeV. The solid curve shows a plot of $(\nu - 1)$ versus turn number n, where ν is the frequency produced exclusively by the magnetic focusing. The broken curve shows a corresponding plot of $(\nu_z - 1)$ versus n, where ν_z is the frequency resulting from the combined effect of both electric and magnetic focusing. Within the stopband, which extends from $n = 4$ to $n = 8.6$, only the value of μ is plotted, where μ is the imaginary part of $(\nu_z - 1)$. The values of μ determine the rate of growth within the stopband, and therefore measure the strength of the instability generated by the electric focusing.

obtain $G = 4.8$, which is a surprisingly large growth factor considering that the stop band acts only over the first 4.6 turns. Of course, after the beam traverses the stop band, the exponential growth ceases.

Since the foregoing calculations assume $\phi = 0$, additional results were obtained using Eq. (25) for different ϕ values. These results show that G decreases rather slowly as ϕ increases. For example, when ϕ goes from zero to 60°, G drops from 4.8 down to 2.7, and although this is a definite improvement, it comes at the cost of decreasing the energy gain per turn by a factor of two.

Only the case with $h = 8$ has been treated here, and we expect that the problem will be still greater for $h = 11$ and 17, since the AG effect is even stronger in these cases. Unfortunately, beam measurements suitable for testing the theory are not yet available, but cyclotron operation on these particular harmonics is indeed quite difficult, and although reliable beams have finally been obtained for $h = 8$, only intermittent operation is as yet possible for $h = 11$ and 17.*

6. MODIFIED DUTTO-CRADDOCK FORMULA

We now proceed to derive the Dutto-Craddock[5] formula, following their general procedure except for certain modifications. First, we use polar rather than Cartesian coordinates, assuming that the central ray moves along a circular arc across the electric gap rather than a straight line. In addition, we do not restrict the time dependence of the electric field to being sinusoidal, but rather allow it to be any function of $\omega_{rf}t$. We also include the possibility that the electric field may not be tangent to the central ray, since this is often the case.

We start by considering one particular gap-crossing. Writing $\mathbf{F} = q\mathbf{E}(r, \theta, z, t)$ for the electric force, we then have

$$\delta p_r = \int F_r dt \,, \tag{30}$$

$$\frac{\delta p_x}{x} = \int \frac{\partial F_r}{\partial r} dt \,, \tag{31}$$

and

$$\frac{\delta p_z}{z} = \int \frac{\partial F_z}{\partial z} dt \,, \tag{32}$$

where δp_r is the radial impulse imparted to the central ray during the gap-crossing, while δp_x and δp_z are the additional impulses imparted to those parallel rays having a small x and z displacement, respectively.

These integrals are evaluated along the central ray for which $r = \text{const.}$, and $dt = d\theta/\omega$. Combining these integrals, we then obtain

$$\frac{\delta p_z}{z} + \frac{\delta p_x}{x} + \frac{\delta p_r}{r} = \int \left(div\mathbf{F} - \frac{1}{r}\frac{\partial F_\theta}{\partial \theta} \right) \frac{d\theta}{\omega} \,,$$

$$= \frac{-1}{v} \int \frac{\partial F_\theta}{\partial \theta} d\theta \,, \tag{33}$$

* We are indebted to R. Pollock, D. Friesel, and J. Dreisbach for providing the data used in this section, and for discussing the relevant beam observations.

since $div\mathbf{F} = q(div\mathbf{E}) = 0$ for the rf electric field inside the gap, and since $v = \omega r$.

In order to evaluate the last integral, we need to make use of the total derivative

$$\frac{dF_\theta}{d\theta} = \frac{\partial F_\theta}{\partial \theta} + \frac{\partial F_\theta}{\partial t}\frac{1}{\omega} + \frac{\partial F_\theta}{\partial r}\frac{dr}{d\theta},$$

$$= \frac{\partial F_\theta}{\partial \theta} + h\frac{\partial F_\theta}{\partial \phi}, \tag{34}$$

since $(dr/d\theta) = 0$ for the central ray, and since $d\phi = \omega_{rf}dt = h\omega dt$ when $d\theta = 0$.

Next we integrate the last equation over θ, choosing as our integration limits values that span the particular gap under consideration. We thereby obtain

$$0 = \int \frac{\partial F_\theta}{\partial \theta} d\theta + h\frac{\partial}{\partial \phi}\int F_\theta d\theta, \tag{35}$$

where the left side vanishes since we may justifiably take $F_\theta = 0$ before the orbit enters the gap and after it exists. That is, we can choose the integration limits midway between successive gap-crossings.

Recognizing that F_θ is the component along the orbit, we therefore write the energy gained during the gap crossing as

$$\delta T = r\int F_\theta d\theta. \tag{36}$$

We now combine this with Eqs. (33) and (35) above to obtain finally

$$\frac{\delta p_z}{m\omega z} + \frac{\delta p_x}{m\omega x} + \frac{\delta p_r}{p} = \frac{h}{2T_c}\frac{\partial}{\partial \phi}(\delta T), \tag{37}$$

where $p = m\omega r$ and $T_c = \frac{1}{2}mv^2$ are evaluated at the center of the gap.

This then is the modified Dutto-Craddock formula, and we see that it reduces to Eq. (14) used in Sec. 3 when $\delta p_x = \delta p_r = 0$. This situation commonly occurs when the dee angle D and the angular width of the gaps are all constants independent of r. In such cases, the median-plane equipotential curves correspond to the radial lines $\theta = \text{const.}$, so that E_θ is the only non-vanishing component of the field in the median plane.

As noted before, the right-hand side of Eq. (37) does not depend on the details of the spatial variation of the electric field within the gap. This implies a complementary relationship between the changes in the radial and vertical focusing, as pointed out by Dutto and Craddock.[5] That is, if the electrode structures defining the gap are deformed in such a way as to increase the vertical focusing, then they must necessarily decrease the radial focusing at the same time.

This complementary relationship is revealed more clearly in the limit where the electric focusing is sufficiently weak so that the method of "averaging" can be applied. In this limit, the change in ν_z^2 is given by

$$\Delta\nu_z^2 = \frac{-1}{2\pi}\sum\left(\frac{\delta p_z}{m\omega z}\right)_j, \tag{38}$$

where the sum here covers all the gaps in one turn. Similarly, we also have

$$\Delta\nu_r^2 = \frac{-1}{2\pi}\sum\left(\frac{\delta p_x}{m\omega x}\right)_j. \tag{39}$$

Hence, summing Eq. (37) over all the gaps in one turn, we finally obtain

$$\Delta\nu_z^2 + \Delta\nu_r^2 = \frac{-h}{4\pi T_0}\frac{\partial}{\partial \phi}(\Delta T) + \frac{1}{2\pi}\sum(\delta p_r/p)_j, \tag{40}$$

where ΔT is the total energy gain per turn, and where T_0 here is the average kinetic energy during the turn.

When the electric-gap lines have no spiral or other curvature, as is true in most cases, the sum on the right vanishes. The complementary relationship then reduces to

$$\Delta\nu_z^2 + \Delta\nu_r^2 = \frac{-h}{4\pi T_0}\frac{\partial}{\partial \phi}(\Delta T). \tag{41}$$

This result also represents a generalization of a similar equation obtained by Dutto and Craddock.

We should emphasize once more that this result applies to any dee geometry because it does not depend on the number of dees N_d nor on their angle D. Moreover, it can also be applied to rf systems containing harmonics of the main frequency, such as those which attempt to simulate the effect of a square-wave voltage.[15]

In the usual case where the energy gain per

turn ΔT is given by Eq. (2), this relationship reduces to

$$\Delta\nu_z^2 + \Delta\nu_r^2 = \frac{h}{4\pi n}\sin\phi\ , \qquad (42)$$

where the turn number n is again defined by Eq. (17). As one would expect, when $\Delta\nu_r^2 = 0$, this result reduces to the one given by the first term in Eq. (23), which does indeed correspond to the weak-focusing limit.

7. SPIRAL ELECTRIC GAPS

Dees with spiral electric gaps form an essential part of the rf systems in superconducting cyclotrons like those being built at Chalk River[16] and at MSU.[10] The effect of such gaps on the variation of the phase ϕ has been discussed in a previous paper[17] and we now wish to examine how these gaps modify the values of both ν_r and ν_z.

In addition to showing a sketch of the three spiral dees in the MSU cyclotron, Fig. 2 also indicates the direction of the electric force **F** at one particular gap-crossing. If α is the angle between this force and the direction of the ion's velocity, then the radial impulse is given by

$$\delta p_r = \delta p_\theta \tan\alpha = (\delta T/v)\tan\alpha\ , \qquad (43)$$

where δT is the energy gained by the ion at this gap.

The dees are required to fit in the magnet valleys between the three spiral pole tips, and this fixes the dee geometry. The spiral turns out to be nearly linear, and can therefore be represented as

$$\tan\alpha = +r/r_s\ , \qquad (44)$$

with $r_s = 13$ in. in our case.

But, this spiral tends to disappear at small radii, and effectively vanishes for $r < 2.5$ in. In addition, we have already seen that the electric focusing strength falls off rapidly with increasing r. As a result, we may justifiably treat the additional focusing effect of the spiral gaps as a weak perturbation.

Inserting the above value of δp_r into Eq. (40). and making use of the definitions for ΔT and n in Eqs. (2, 17), we finally obtain

$$\Delta\nu_z^2 + \Delta\nu_r^2 = \frac{1}{4\pi n}(h\sin\phi + \tan\alpha\cos\phi)\ . \qquad (45)$$

This equation, which is the analogue of Eq. (42), now represents the complementary relationship between the radial and vertical focusing for the case of spiral electric gaps.

We turn next to evaluate the effect on the radial focusing by itself. Starting from Eq. (31) for δp_x, and using Eq. (30) for δp_r, we then find

$$(\delta p_x)/x = (\partial/\partial r)\delta p_r = (\delta T/v)(\partial/\partial r)\tan\alpha. \qquad (46)$$

For the special case of linear spiral, as in Eq. (44) above, this result can be reduced to

$$\frac{\delta p_x}{m\omega x} = \frac{\delta T}{pv}\tan\alpha\ , \qquad (47)$$

which, by comparison with (43), is evidently the same as $\delta p_r/p$.

For the spiral shown in Fig. 2, the quantities α, δp_r, and δp_x are all positive, and the spiral gaps therefore produce radial defocusing. Clearly, if the spiral direction were reversed, then radial focusing would be produced.

Since the focusing here is weak, we can use Eq. (39) to evaluate $\Delta\nu_r^2$. Thus, following the same steps that led to Eq. (45) above, we finally obtain

$$\Delta\nu_r^2 = -\left(\frac{\tan\alpha}{4\pi n}\right)\cos\phi\ . \qquad (48)$$

In addition, inserting this result into Eq. (45) above then leads to

$$\Delta'\nu_z^2 = +2\left(\frac{\tan\alpha}{4\pi n}\right)\cos\phi = -2\Delta\nu_r^2\ , \qquad (49)$$

where $\Delta'\nu_z^2$ here represents the change in ν_z^2 when the ordinary electric focusing is omitted. These two equations therefore describe the specific effect of the spiral gaps on the radial and vertical focusing considered individually.

For the MSU cyclotron, the relation (28) between n and r can be rewritten most conveniently as

$$n = n_f(r/r_f)^2\ , \qquad (50)$$

where the final orbit radius $r_f = 26$ in. is nearly fixed, while the final turn number n_f varies from 130 to 560 depending on operating conditions.

With $\tan\alpha = r/r_s$ in our case, we then find that $\Delta\nu_r^2$ in (48) falls off as $1/r$, at least for $r > 2.5$ in. Moreover, since the spiral effectively vanishes

inside this radius, the maximum value of $\Delta\nu_r^2$ will occur at around $r = 2.5$ in.

Putting the numerical information together, and setting $\phi = 0$ for simplicity, we then obtain

$$\Delta\nu_r^2 = -0.013(130/n_f)(2.5/r), \qquad (51)$$

where $n_f > 130$ and $r > 2.5$ in., as noted above.

For the MSU cyclotron, it has also been determined that when only magnetic focusing is considered, the resultant ν_r values start out at around 0.99, and then rise slowly through $\nu_r = 1$ at about $r = 4$ in. Thus, since $\nu_r \simeq 1$ for the small r values of interest here, we may use a first-order expansion to solve Eq. (48) and we thereby obtain

$$\nu_r^* = \nu_r - 0.0065(130/n_f)(2.5/r), \qquad (52)$$

where ν_r^* is the resultant focusing frequency including the effect of spiral gaps. We may therefore conclude that the main effect will be a slight shift in the location of the $\nu_r = 1$ resonance, and it seems quite unlikely that this shift will produce any detectable consequences.

Returning now to the vertical focusing, and substituting the given data into Eq. (49), we now find

$$\Delta'\nu_z^2 = +0.026(130/n_f)(2.5/r)\cos\phi. \qquad (53)$$

Apparently, the change in ν_z produced by the spiral gaps could be quite significant in certain cases. For example, in the region between $r = 2.5$ and 5.0 in., we expect that ν_z would lie between 0.1 and 0.2 if the spiral-gap effect were absent. But when this effect is included, we find that the values of ν_z may be increased sufficiently so as to lie between 0.19 and 0.26.

As mentioned above, reversing the direction of the spiral gaps also reverses their focusing effect. In our case, this reversal would produce a net increase in ν_r and a net decrease in ν_z. Judging from the above results, the direction of the change in ν_r would not matter much. However, it should be quite evident that a decrease in ν_z of the magnitude indicated above could produce very serious problems.

As is well known, magnetic focusing is completely independent of the direction of the spiral. Moreover, since the focusing effect of the spiral gaps was not considered during the design of the MSU cyclotron, the final choice of the spiral direction was based entirely on other considerations. Fortunately, this choice (shown in Fig. 2) turns out to be the correct one with respect to focusing since it increases ν_z rather than decreasing it.

REFERENCES

1. M.E. Rose, *Phys. Rev.* **53,** 392 (1938).
2. R.R. Wilson, *Phys. Rev.* **53,** 408 (1938).
3. B.L. Cohen, *Rev. Sci. Instr.* **24,** 589 (1953).
4. P. Kramer, H.L. Hagedoorn, and N.F. Verster, *International Conference on Sector-focused Cyclotrons and Meson Factories,* (CERN, Geneva, 1963), p. 214. R. Cohen and J. Rainwater, *IEEE Trans. Nucl. Sci.* **NS-16,** 426 (1969). M. Reiser, *J. Appl. Phys.* **42,** 4128 (1971).
5. G. Dutto, and M.K. Craddock, *Proc. 7th Int. Conf. on Cyclotrons and their Applications,* (Birkhauser, Basel, 1975), p. 271.
6. M. Reiser, *Nucl. Instrum. Methods* **13,** 55 (1961). H.G. Blosser, *5th Int. Cyclotron Conf.,* (Butterworths, London, 1971), p. 257. G. Dutto et al., *Proc. 6th Int. Cyclotron Conf.* (AIP, New York, 1972), p. 340. J.I.M. Botman, H.L. Hagedoorn, and W.M. Van der Ligt, *Nucl. Instrum. Methods* **171,** 201 (1980).
7. J.A. Martin, *IEEE Trans. Nucl. Sci.* **NS-26,** 2443 (1979).
8. M.S. Livingston, *The Development of High Energy Accelerators* (Dover, New York, 1966), section III.
9. A.A. Kolomensky and A.N. Lebedev, *Theory of Cyclic Accelerators* (North Holland, Amsterdam, 1966), Ch. 4.
10. H.G. Blosser, *IEEE Trans. Nucl. Sci.* **NS-26,** 2040 (1979).
11. E. Liukkonen, J. Bishop, S. Motzny, and T. Antaya, *IEEE Trans. Nucl. Sci.* **NS-26,** 2107 (1979).
12 R.E. Pollock, *IEEE Trans. Nucl. Sci.* **NS-26,** 1965 (1979).
13. M.M. Gordon, *Ann. Phys.* **50,** 571 (1968).
14. B.M. Bardin, J.H. Hettmer, W.P. Jones, and C.J. Kost, *IEEE Trans. Nucl. Sci.* **NS-18,** 311 (1971).
15. M.M. Gordon, *Particle Accelerators* **2,** 203 (1971).
16. J.H. Ormrod *et al., IEEE Trans. Nucl. Sci.* **NS-26,** 2034 (1979).
17. M.M. Gordon, *Nucl. Instrum. Methods* **169,** 327 (1980).